Computational quantitative flow ratio to assess functional severity of coronary artery stenosis

Ties, Daan; van Dijk, Randy; Pundziute, Gabija; Lipsic, Erik; Vonck, Ton E; van den Heuvel, Ad F M; Vliegenthart, Rozemarijn; Oudkerk, Matthijs; van der Harst, Pim

IMPORTANT NOTE: You are advised to consult the publisher's version (publisher's PDF) if you wish to cite from it. Please check the document version below.

Document Version
Publisher's PDF, also known as Version of record

Link to publication in University of Groningen/UMCG research database
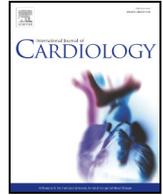
Computational quantitative flow ratio to assess functional severity of coronary artery stenosis

Daan Ties [a,b], Randy van Dijk [a,b], Gabija Pundziute [b], Erik Lipsic [b], Ton E. Vonck [b], Ad F.M. van den Heuvel [b], Rozemarijn Vliegenthart [a,c], Matthijs Oudkerk [a], Pim van der Harst [a,b,*]

[a] University of Groningen, University Medical Center Groningen, Center for Medical Imaging, Groningen, The Netherlands
[b] University of Groningen, University Medical Center Groningen, Department of Cardiology, Groningen, The Netherlands
[c] University of Groningen, University Medical Center Groningen, Department of Radiology, Groningen, The Netherlands

ABSTRACT

Background: Computational quantitative flow ratio (QFR) based on 3-dimensional quantitative coronary angiography (3D QCA) analysis offers the opportunity to assess the significance of coronary artery disease (CAD) without using an invasive pressure wire or inducing hyperemia. This study aimed to evaluate the diagnostic performance of QFR compared to wire-based fractional flow reserve (FFR) and to validate the previously reported QFR cut-off value of >0.90 to safely rule out functionally significant CAD.
Methods: QFR was retrospectively derived from standard-care coronary angiograms. Correlation and agreement of fixed-flow QFR (fQFR) and contrast-flow QFR (cQFR) models with invasive wire-based FFR was calculated. Diagnostic performance of QFR was evaluated at different QFR cut-off values defining significant CAD (FFR ≤ 0.80).
Results: 101 vessels in 96 patients who underwent FFR were studied. Mean FFR was 0.87 ± 0.08 and 21 of 101 (21%) vessels had an FFR ≤ 0.80. Correlation of fQFR and cQFR with FFR was $r = 0.71$ ($p < 0.001$) and $r = 0.70$ ($p < 0.001$), respectively. Sensitivity and specificity were 57% and 93% for fQFR and 67% and 96% for cQFR at a QFR cut-off value >0.80 defining non-significant CAD, respectively. fQFR > 0.90 was present in 34 (34%) and cQFR > 0.90 in 39 (39%) vessels. For both QFR models, none of the vessels with QFR > 0.90 had an FFR ≤ 0.80.
Conclusions: QFR appears to be a safe and effective gatekeeper to wire-based FFR when applying a QFR threshold of >0.90 to rule out significant CAD. Further prospective research is required to establish QFR in the real-life setting of functional CAD assessment in the catheterization laboratory.

1. Introduction

Coronary artery disease (CAD) is the most common cause of death globally, resulting in 8.9 million deaths annually worldwide [1]. The clinical relevance of CAD can be assessed by visual inspection of the anatomical stenosis on the coronary angiogram [2] or by measuring its functional consequence using fractional flow reserve (FFR) [3] or instantaneous wave-free ratio (iFR) [4,5]. Functional assessment of CAD by FFR was shown to be superior to visual assessment for therapy decision-making [6]. To determine FFR, the introduction of an invasive pressure wire and induction of hyperemia is required, increasing patient discomfort, complication risk and costs associated with the catheterization procedure. Tu et al. developed fast quantitative flow ratio (QFR) computation models based on 3-dimensional quantitative coronary angiography (3D QCA) to calculate FFR from angiographic images without introducing an invasive pressure wire in the coronary artery or inducing hyperemia, and showed good agreement of QFR computation models with wire-based FFR [7]. Validation of these first results on QFR analysis is essential in order to prevent inappropriate adjustment of diagnostic strategies based on results of unreproducible studies (Baker, Nature 2016). Our study will explore the diagnostic accuracy of QFR and the potential of QFR to safely rule out haemodynamic relevant coronary artery stenosis by evaluation of various QFR rule-out thresholds. We aim to validate the previously reported QFR cut-off value of >0.90 to safely rule out functionally significant CAD [7].

2. Methods

2.1. Study design

This is a retrospective, single-centre observational study performed in the University Medical Center Groningen, The Netherlands. QFR is compared to the reference standard of FFR. The medical ethics review board of the University Medical Center Groningen reviewed the protocol (METc 2016/455). None of the patients objected to the use of their medical data for scientific research.

* Corresponding author at: University of Groningen, University Medical Center Groningen, Hanzeplein 1 (AB31), 9713GZ Groningen, The Netherlands.
E-mail address: p.van.der.harst@umcg.nl (P. van der Harst).

2.2. Study population

Coronary angiograms of all patients in whom FFR was performed in the UMCG as part of routine clinical care in the period between January 2015 and July 2015 were screened for further analysis by dedicated QFR software (QAngio XA 3D/QFR research version 1.0.28.0, Medis Medical Imaging Systems, Leiden, The Netherlands). In- and exclusion criteria of angiograms were based on practical requirements of QFR software. Inclusion criteria were: 1) documentation of the exact wire-based FFR values, 2) availability of two angiogram acquisitions of the interrogated vessel, 3) an angle ≥25° between the two angiogram acquisitions of one vessel and 4) perpendicularity of both acquisitions towards the interrogated vessel. Exclusion criteria were: 1) no documented nitroglycerine administration prior to the recording of acquisitions, 2) image acquisition speed of <10 frames/s, 3) prior coronary artery bypass grafting (CABG) on the interrogated vessel 4) true bifurcation lesion (1-1-1 according to Medina classification), 5) ostial left main or ostial right coronary artery lesion, 6) retrograde filling of the interrogated vessel, 7) hyperdynamic heart.

2.3. Enrolment of cases

QFR was retrospectively derived from standard-care coronary angiograms. Although acquisitions were of sufficient quality for clinical decision making, not all acquisitions met the software requirements for standardized views and adequate contrast injection. Four known analysis-complicating factors were scored: degree of vessel overlap (0 = none, 1 = moderate, 2 = severe), degree of foreshortening (0 = none, 1 = moderate, 2 = severe), general image quality/brightness (0 = none, 1 = moderate, 2 = bad) and quality of contrast agent injection (0 = fast/brisk, 1 = slow/stagnating). An Image Quality Score (IQS) was calculated on a per-vessel basis by summing up the scores per factor for the two acquisitions separately. Vessels with IQS ≥3 for one of the two acquisitions were considered inappropriate for QFR calculation and excluded from further analysis.

2.4. Image collection

Coronary angiogram acquisitions of patients were collected from the Picture Archiving and Communication System (PACS). All patients received an individual study-specific code. When the inclusion criteria were met, the appropriate acquisitions were selected and stored separately from the rest of the acquisitions. Final QFR analysis was performed on these separately stored acquisitions one week later to ensure readers were blinded for possibly performed interventions visible on acquisitions encountered during the selection process. Coronary angiogram acquisitions were recorded with a frame acquisition speed of 10 or 15 frames per second.

2.5. QFR analysis

Offline QFR analysis was performed by a trained (Level 2 Certification, Medis Medical Imaging Systems) reader. A second trained reader was consulted in case execution of QFR analysis was troublesome. All readers were blinded to the wire-based FFR values. The vessel in which FFR was performed was known to the reader. To avoid excessive compression of the interrogated vessel, end-diastolic frames were selected. End-diastolic phase was defined by the presence of maximal myocardial relaxation on the acquisition frame in combination with end of P-wave on the electrocardiographic signal, when available. Setpoints for segment selection were placed at the ostium of the interrogated vessel proximally and at the location of the proximal tip of the FFR pressure sensor distally in order to conduct QFR analysis in accordance with the original FFR procedure. To match vessel contours, side branches were indicated as corresponding anatomical landmarks on both acquisitions. Vessel contours were automatically detected on the two acquisitions and manually adjusted in case of erroneous registration or side branch disturbance. Based on the corresponding 2D acquisitions, a 3D reconstruction of the single coronary vessel was generated by the QFR software. Bifurcation lesions were analysed as single vessels without side branches. 3D QCA percent diameter stenosis (DS) and percent area stenosis (AS) were derived from the 3D model of the vessel and calibration data saved in the DICOM files of acquisitions. Fixed-flow QFR (fQFR) and contrast-flow QFR (cQFR) were calculated by the software, as previously described [7,8]. In brief, pressure drop is calculated using a quadratic equitation incorporating vessel geometry and hyperemic flow velocity (HFV). fQFR is calculated using a fixed experiential HFV of 0.35 m/s, based on a previous study [8]. cQFR is calculated using a modelled HFV, derived from frame counting on contrast-enhanced images acquired at rest. Frame counting is manually performed by indicating the acquisition frame at which the contrast bolus reaches proximal and distal limits of the analysed segment. Fig. S1 shows an overview of the practical execution of QFR analysis.

2.6. FFR

Blood pressures were measured at the catheter tip and distally from the stenosis using PressureWire Aeris (St. Jude Medical Systems, Saint Paul, Minnesota, United States). A bolus of 200–400 μg nitroglycerin was administered intracoronary prior to measurements. A dose of 120 μg adenosine was administered intracoronary to induce hyperaemia. In case of sequential lesions adenosine was administered intravenously (140 μg/kg/min). After reaching minimal FFR value distally, the pressure wire was pulled back across the vessel to assess pressure drop across single lesions. To calculate FFR, mean distal coronary pressure was divided by mean aortic pressure.

2.7. Statistical analysis

Categorical variables are shown as a number and percentage. Continuous variables are described by mean ± SD or median (interquartile range) in case of non-normal distribution. Wire-based FFR was defined as the reference standard. An FFR threshold of ≤0.80 was used to define significant CAD. Pearson correlation coefficient (r) was calculated to quantify the correlation of QFR models with wire-based FFR and Spearman correlation coefficient (ρ) was calculated to quantify correlation of 3D QCA parameters with FFR. Bland Altman analysis was used to determine agreement of QFR models with FFR. The diagnostic performance of QFR and 3D QCA was evaluated by describing diagnostic accuracy, sensitivity, specificity, positive predictive value (PPV) and negative predictive value (NPV). A common 3D QCA DS cut-off value of ≥50% and optimal Youden Index AS cut-off value of ≥63.5% was used to define significant coronary stenosis. To evaluate the potential use of QFR as a gatekeeper to FFR, we determined the diagnostic performance of both the optimal QFR cut-off value in our study population (as determined by the Youden Index) and the previously reported QFR cut-off value of >0.90 defining non-significant CAD. [7] The area under the receiver operating characteristic curves (AUC) were compared using the DeLong method. Statistical significance was defined as a two-sided p-value of <0.05. Statistical analysis was performed using SPSS (IBM SPSS Statistics version 23.0, Chicago, United States). Receiver operating characteristic curve analysis was performed using Stata (StataCorp LP, StataMP version 13.0, College Station, United States).

3. Results

3.1. Patient and lesion characteristics

274 patients with 333 vessels were screened for inclusion. A total of 128 patients with 133 vessels met basic in- and exclusion criteria. Seventeen vessels had IQS ≥3 and were excluded. Fifteen additional vessels were excluded after 2 readers reached consensus about inadequateness of acquisitions caused by factors not reflected by the IQS. The final study population consisted of 96 patients and 101 coronary vessels. Fig. 1 shows an overview of patient and vessel selection. Patient characteristics are shown in Table 1. Lesion characteristics are shown in Table S1. The mean FFR was 0.87 ± 0.08. In 21 of 101 vessels, the lesion caused an FFR ≤ 0.80.

3.2. Correlation and agreement of QFR and 3D QCA with FFR

The correlation of fQFR and cQFR with wire-based FFR was $r = 0.71$ ($p < 0.001$) and $r = 0.70$ ($p < 0.001$), respectively (Fig. S2). For 3D QCA DS and AS, correlation with wire-based FFR was $\rho = -0.47$ ($p < 0.001$) and $\rho = -0.37$ ($p < 0.001$), respectively (Fig. S3). The mean difference with wire-based FFR was 0.003 ± 0.06 ($p = 0.39$) for fQFR and -0.001 ± 0.06 ($p = 0.64$) for cQFR (Fig. S2).

3.3. Diagnostic performance of QFR compared to 3D QCA

Accuracy, sensitivity, specificity, PPV and NPV were 85%, 57%, 93%, 67%, and 89% for fQFR and 90%, 67%, 96%, 82%, and 92% for cQFR at a QFR cut-off value of >0.80, respectively. Accuracy, sensitivity, specificity, PPV and NPV were 75%, 43%, 84%, 41%, and 85% for DS and 74%, 67%, 76%, 42%, and 90% for AS, respectively. AUC was significantly larger for fQFR (AUC 0.92) compared to 3D QCA DS (AUC 0.79, difference; 0.13, $p < 0.001$) and AS (AUC 0.74, difference; 0.18, $p < 0.001$) and significantly larger for cQFR (AUC 0.92) compared to 3D QCA DS (AUC 0.79, difference; 0.13, $p < 0.001$) and AS (AUC 0.74, difference; 0.18, $p < 0.001$) (Fig. 2).

3.4. Diagnostic performance of QFR at optimal QFR thresholds

The optimal QFR cut-off was >0.83 for fQFR and >0.82 for cQFR in our study population. At optimal QFR cut-offs, 2 and 5 vessels were falsely indicated as non-obstructive by fQFR and cQFR, respectively. Accuracy, sensitivity, specificity, PPV and NPV were 80%, 90%, 78%, 51% and 97% for fQFR and 87%, 76%, 90%, 67% and 94% for cQFR at these QFR cut-offs, respectively, as shown in Table 2.
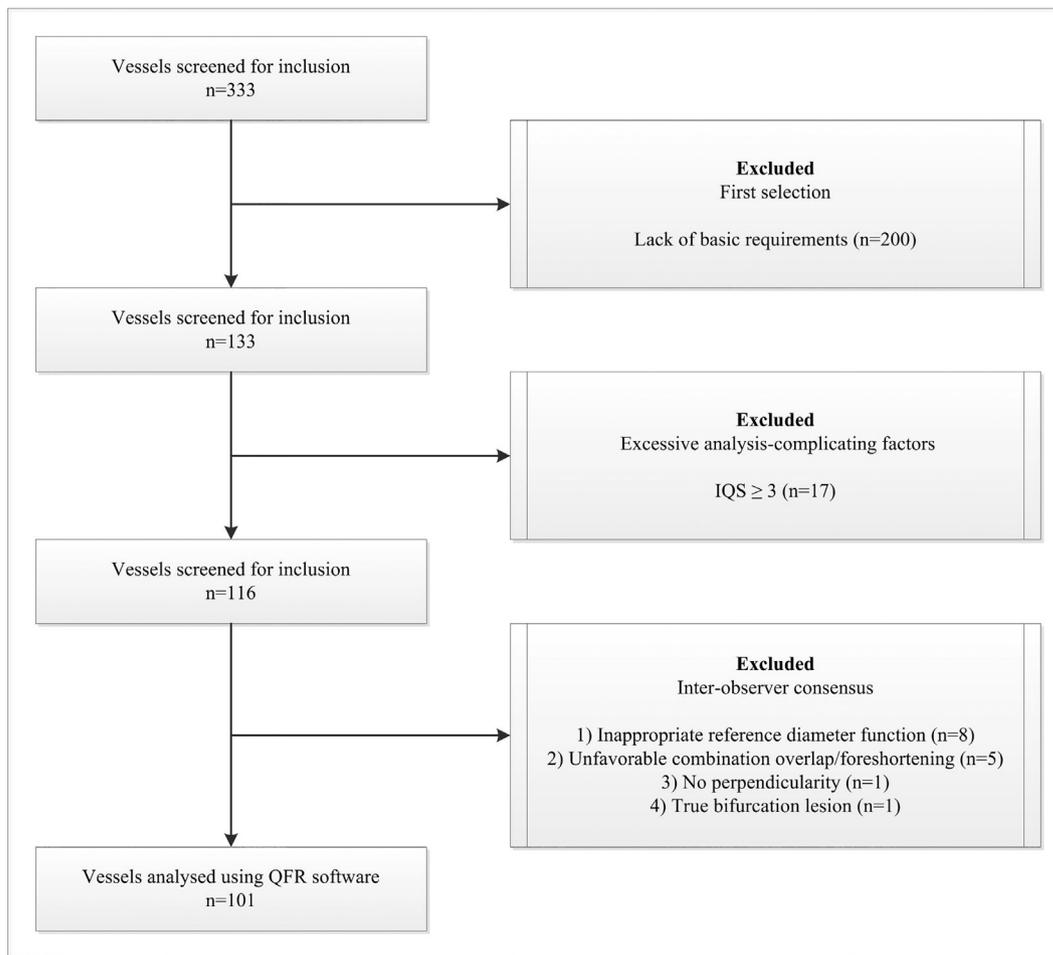
Fig. 1. Patient and vessel selection. QFR = quantitative flow ratio; IQS = image quality score.

3.5. Validation of QFR cut-off >0.90

None of the vessels with QFR >0.90 had a wire-based FFR value of ≤0.80 for both QFR models. Accuracy, sensitivity, specificity, PPV and NPV were 54%, 100%, 43%, 31% and 100% for fQFR and 59%, 100%, 49%, 34% and 100% for cQFR at these QFR cut-offs, respectively, as shown in Table 2. QFR was >0.90 in 34 (34%) and 39 (39%) of the evaluated vessels for fQFR and cQFR, respectively.

4. Discussion

We observed that computational fQFR and cQFR have good diagnostic performance compared to wire-based FFR, and superior diagnostic performance compared to 3D QCA analysis. In our study population, a QFR threshold of >0.90 could safely rule out functionally significant stenosis and has the potential to reduce the number of wire-based FFR procedures at the catheterization laboratory with 34–39%. However, large prospective trials comparing clinical outcomes of patients deferred for revascularisation based on FFR versus QFR are necessary for QFR to be implemented in daily clinical practice.

One of the most promising applications of computational QFR is the potential to use the technique as a gatekeeper to wire-based FFR for the functional assessment of intermediate coronary stenosis, hereby possibly reducing complication risk and costs associated with introduction of sophisticated pressure wires. Previously, Tu et al. studied the diagnostic performance of QFR, and reported a QFR threshold of >0.90 to safely rule out functionally significant CAD [7]. The limitations of this previous work included the small sample size and lack of data on QFR analysis

Table 1
Patient characteristics.

Patient characteristics	n = 96
Age (year)	63.9 ± 10.3
Gender	
Male	58 (60.4)
Body mass index (kg/m²)[a]	27.3 ± 5.1
Smoking[b]	
Current	26 (28.6)
Former	22 (24.2)
Never	43 (47.3)
Hypertension	68 (70.8)
Hyperlipidemia	70 (72.9)
Diabetes mellitus	24 (25.0)
Family history of CVD[b]	42 (46.2)
Indication for procedure	
Stable CAD	49 (51.0)
Unstable CAD	15 (15.6)
NSTEMI	16 (16.7)
Non-culprit evaluation	16 (16.7)
Prior PCI	23 (24.0)
Prior CABG	3 (3.1)

Values are expressed as n (%) or mean ± SD. CABG = coronary artery bypass grafting; CAD = coronary artery disease; CVD = cardiovascular disease; NSTEMI = non-ST elevation myocardial infarction; PCI = percutaneous coronary intervention.

  [a] Data missing in 13 patients.
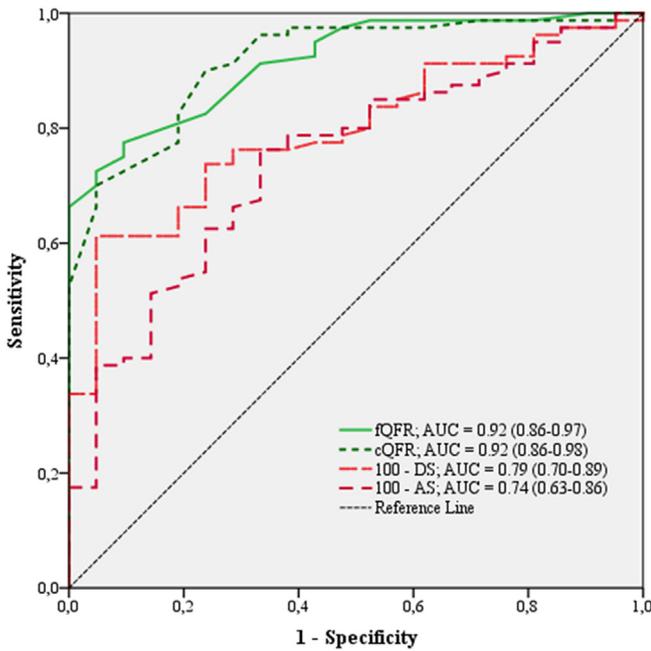 [b] Data missing in 5 patients.

Fig. 2. Receiver operating characteristic curves of functional QFR models compared to anatomical 3D QCA parameters. The AUC was significantly larger for both fQFR and cQFR compared to 3D QCA DS and AS. 3D QCA = 3-dimensional quantitative coronary angiography; AS = percent area stenosis; AUC = Area under the receiver operating characteristic curve; cQFR = contrast-flow quantitative flow ratio; DS = percent diameter stenosis; fQFR = fixed-flow quantitative flow ratio; QFR = quantitative flow ratio.

performed outside a dedicated core laboratory. Extensive validation before moving on to clinical application is essential to ensure safety in real-life setting. We now studied a larger European population in which none of the vessels with QFR > 0.90 had an FFR ≤ 0.80. We provide the first independent data confirming the QFR threshold of >0.90 as a safe rule out threshold to exclude significant CAD. The next step necessary to implement QFR in daily clinical practice will be to instantly assess QFR during diagnostic angiography in the catheterization laboratory. Online QFR, which became available after execution of this study and is currently under investigation, will allow for this rapid QFR assessment during diagnostic angiography. In our study, the time to perform QFR analysis was approximately 5–10 min. Online QFR also features an image acquisition guide to support adequate recording of acquisitions for QFR analysis, which will enhance clinical practicability of QFR. We believe that online QFR analysis is a feasible approach to reduce the number of expensive invasive wire-based FFR procedures.

This study also showed that QFR computation is more accurate in determining the significance of coronary artery stenosis compared to 3D QCA analysis. AUC was larger for both QFR models as compared to AUC for both 3D QCA DS and AS. These findings are in line with a study by Tu et al. comparing diagnostic performance of computational FFR with 3D QCA [8].

4.1. Limitations of QFR analysis

Several requirements must be met to accurately and rapidly perform QFR analysis. Manual indication of anatomical landmarks, selection of start/endpoint of vessel segment to be analysed, and correction of vessel contouring are user interactions that might affect QFR results. QFR was shown to have good inter-observer agreement [9], but training of medical staff is essential to ensure high-quality and reliable execution of online QFR analysis.

QFR dependency on defining a reference diameter function of the analysed vessel to estimate stenosis dimensions [7] is limiting its use in several cases. The limited availability of proximal disease-free vessel in lesions near the origin of the vessel causes underestimation of proximal reference diameter. In diffusely diseased or ectatic vessels, the diminished presence of healthy coronary artery segments overestimates the reference diameter function. "Flagging" was applied to ignore unrepresentative segments in reference diameter function simulation, but the effect of this correction method on QFR reliability remains unclear.

A 3D model of the coronary vessel based on two 2D coronary angiogram acquisitions is reconstructed to estimate stenosis and vessel geometry. Although 2 points of view are used, part of the actual vessel and stenosis remains unknown. Unequal distribution of plaque along the vessel wall in eccentric plaques [10] might result in false assumptions on stenosis geometry, possibly affecting accuracy of QFR in this specific kind of plaques.

Cases with previous CABG on the interrogated vessel were excluded in our study based on recommendations by the QFR software vendor. No recommendations on cases with previous percutaneous coronary intervention (PCI) were made and cases with previous PCI were included. We hypothesize that the presence of stent material influences QFR analysis. A study by Gutiérrez-Chico et al. [11] comparing different methods for quantification of stented vessel dimensions showed that QCA consistently underestimates both stent length as minimal lumen area after stent placement. Stent material might alter the vascular dimensions influencing vessel contouring. Due to low numbers in the group with previous PCI, we were unable to study the influence of stent material on accuracy of QFR analysis.

Finally, the influence of bifurcation lesions on coronary flow distribution and velocity was ignored due to the fact that the QFR software

Table 2
Diagnostic performance of QFR at various cut-off values ruling out significant stenosis.

Index test	TP	FN	TN	FP	Accuracy	Sensitivity	Specificity	PPV	NPV
fQFR									
>0.80	12	9	74	6	85 (77–91)	57 (34–78)	93 (84–97)	67 (41–87)	89 (80–95)
>0.83	19	2	62	18	80 (71–87)	90 (70–99)	78 (67–86)	51 (34–68)	97 (89–100)
>0.90	21	0	34	46	54 (44–64)	100 (84–100)	43 (32–54)	31 (21–44)	100 (90–100)
cQFF									
>0.80	14	7	77	3	90 (83–95)	67 (43–85)	96 (89–99)	82 (57–96)	92 (84–97)
>0.82	16	5	72	8	87 (79–93)	76 (53–92)	90 (81–96)	67 (45–84)	94 (85–98)
>0.90	21	0	39	41	59 (49–69)	100 (84–100)	49 (37–60)	34 (22–47)	100 (91–100)

An FFR ≤ 0.80 was used as reference standard defining significant stenosis. Values are presented as either n or % (95% confidence interval). cQFR = contrast-flow quantitative flow ratio; FN = false negatives; FP = false positives; fQFR = fixed-flow quantitative flow ratio; NPV = negative predictive value; PPV = positive predictive value; TN = true negatives; TP = true positives.

did not provide a distinct method for the analysis of bifurcation lesions, possibly making the QFR calculation less accurate in these lesions. Future software developments should focus on solving these problems.

4.2. Study limitations

QFR was retrospectively derived from standard-care coronary angiograms. Coronary angiograms were screened for further analysis by dedicated QFR software and cases with inadequate image quality were excluded. This might have introduced a selection bias in this study, potentially affecting study results.

The mean FFR in our population is higher compared to the typical mean FFR value as previously reported [12]. As discussed above, QFR analysis is impracticable in complex lesions influencing vessel simulation. A study by Takashima et al. [13] showed a significant negative correlation between morphological lesion severity count (presence of eccentric or diffuse lesions, excessive lesion bend or major side branch involvement) and FFR. The exclusion of these complex lesions in our study by means of the IQS or inappropriate reference diameter functions possibly lead to the exclusion of relatively more lesions with low FFR. Although this might have introduced a selection bias into our study, correction for this would have diminished the representation of clinical QFR analysis in our study.

We compared fQFR and cQFR computation models to wire-based FFR. We expected cQFR to have higher accuracy compared to fQFR, because patient-specific frame counting was used for coronary flow velocity estimation in cQFR computation [7]. In our analyses, the overall diagnostic accuracy of cQFR was not superior compared to fQFR. Several aspects might explain this. First, a substantial portion of analysed acquisitions was recorded with a frame acquisition speed of 10 frames/s (to reduce radiation dose), which contains limited additional information and might be insufficient to substantially improve the cQFR calculations. The relatively low frame acquisition speed might also have impeded accurate selection of optimal diastolic images, possibly influencing both fQFR and cQFR calculation. Secondly, cQFR calculation is highly influenced by the degree of briskness and fluency of contrast agent injection. We included the quality of contrast agent injection in the IQS, used to quantify analysis-complicating factors and select appropriate acquisitions, but did not consider adequate contrast agent injection as an individual selection criterion. Therefore, we suggest to use adequate and consistent contrast injection protocols in future prospective studies to test the theoretical superiority of cQFR compared to fQFR.

4.3. Implications

QFR has the potential to prevent patient discomfort associated with adenosine-induced hyperemia, improve patient safety and reduce health care costs when implemented as a gatekeeper to invasive wire-based FFR. Here, we validated the threshold of >0.90 to safely rule out significant CAD. We believe this threshold can be implemented in prospective clinical trials designed to compare clinical outcome of patients deferred for revascularization guided by online QFR versus wire-based FFR. The aspects limiting QFR analysis as indicated in our study should be taken into account when designing prospective trials. Future development and improvement of online QFR focussing on these factors might lead to lowering the QFR threshold, but as long as no large prospective trials are available, the grey zone in which QFR will need to be followed with wire-based FFR to obtain certainty about the best treatment strategy will remain large.

5. Conclusions

Both QFR computation models (fQFR and cQFR) for the functional assessment of CAD showed good overall diagnostic accuracy as compared to invasive wire-based FFR. We validated the proposed threshold of QFR >0.90 to safely rule out significant CAD and suggest that this threshold can be used as a gatekeeper to potentially avoid 34–39% of the invasive wire-based FFR procedures. However, further prospective research is required to provide definitive proof of the diagnostic accuracy of online computational QFR and its safety.

Abbreviations

3D QCA	3-dimensional quantitative coronary angiography
AS	area stenosis
AUC	area under the receiver operating characteristic curve
CAD	coronary artery disease
cQFR	contrast-flow quantitative flow ratio
DS	diameter stenosis
FFR	fractional flow reserve
fQFR	fixed-flow quantitative flow ratio
iFR	instantaneous wave-free ratio
IQS	image quality score
NPV	negative predictive value
PACS	picture archiving and communication system
PPV	positive predictive value
QCA	quantitative coronary angiography
QFR	quantitative flow ratio

Conflict of interest statement

Daan Ties and Randy van Dijk received training from Medis Medical Imaging Systems to perform quantitative flow ratio computation in accordance with the instructions of the manufacturer. The authors report no other relationships that could be construed as a conflict of interest.

Appendix A. Supplementary data

Supplementary data to this article can be found online at https://doi.org/10.1016/j.ijcard.2018.05.002.

References

[1] GBD 2015 Mortality and Causes of Death Collaborators, Global, regional, and national life expectancy, all-cause mortality, and cause-specific mortality for 249 causes of death, 1980–2015: a systematic analysis for the global burden of disease study 2015, Lancet 388 (10053) (2016) 1459–1544.

[2] The Task Force on Myocardial Revascularization of the European Society of Cardiology (ESC) and the European Association for Cardio-Thoracic Surgery (EACTS), 2014 ESC Guidelines on myocardial revascularization, Eur. Heart J. 35 (8) (2014) 1–100.

[3] The Task Force on the management of stable coronary artery disease of the European Society of Cardiology, 2013 ESC guidelines on the management of stable coronary artery disease, Eur. Heart J. 34 (38) (2013) 2949–3003.

[4] M. Götberg, E.H. Christiansen, I.J. Gudmundsdottir, et al., Instantaneous wave-free ratio versus fractional flow reserve to guide PCI, N. Engl. J. Med. 376 (2017) 1813–1823.

[5] J.E. Davies, S. Sen, H.-M. Dehbi, et al., Use of the instantaneous wave-free ratio or fractional flow reserve in PCI, N. Engl. J. Med. 376 (19) (2017) 1824–1834.

[6] P.A.L. Tonino, B. De Bruyne, N.H.J. Pijls, et al., Fractional flow reserve versus angiography for guiding percutaneous coronary intervention, New Engl. J. 360 (3) (2009) 1045–1057.

[7] S. Tu, J. Westra, J. Yang, et al., Diagnostic accuracy of fast computational approaches to derive fractional flow reserve from diagnostic coronary angiography, JACC Cardiovasc. Interv. 9 (19) (2016) 2024–2035.

[8] S. Tu, E. Barbato, Z. Köszegi, et al., Fractional flow reserve calculation from 3-dimensional quantitative coronary angiography and TIMI frame count: a fast computer model to quantify the functional significance of moderately obstructed coronary arteries, JACC Cardiovasc. Interv. 7 (7) (2014) 768–777.

[9]   A.R. van Rosendael, G. Koning, A.C. Dimitriu-Leen, et al., Accuracy and reproducibil-
       ity of fast fractional flow reserve computation from invasive coronary angiography,
       Int. J. Card. Imaging 33 (9) (2017) 1305–1312.
[10] D. Hausmann, A.J.S. Lundkvist, G. Friedrich, K. Sudhir, P.J. Fitzgerald, P.G. Yock,
       Lumen and plaque shape in atherosclerotic coronary arteries assessed by in vivo
       intracoronary ultrasound, Am. J. Cardiol. 74 (9) (1994) 857–863.
[11] J.L. Gutiérrez-Chico, P.W. Serruys, C. Girasis, et al., Quantitative multi-modality imag-
       ing analysis of a fully bioresorbable stent: a head-to-head comparison between QCA,
       IVUS and OCT, Int. J. Card. Imaging 28 (3) (2012) 467–478.
[12] M. Götberg, C.M. Cook, S. Sen, S. Nijjer, J. Escaned, J.E. Davies, The evolving future of
       instantaneous wave-free ratio and fractional flow reserve, J. Am. Coll. Cardiol. 70
       (11) (2017) 1379–1402.
[13] H. Takashima, K. Waseda, M. Gosho, et al., Severity of morphological lesion com-
       plexity affects fractional flow reserve in intermediate coronary stenosis, J. Cardiol.
       66 (3) (2015) 239–245.